16

On the Application of Optimal PWM of Induction Motor in Synchronous Machines at High Power Ratings

Arash Sayyah[1] and Alireza Rezazadeh[2]
[1]*ECE Department, Boston University, Boston, MA*
[2]*ECE Department, Shahid Beheshti University, Tehran*
[1]*USA*
[2]*Iran*

1. Introduction

Distinctive features of synchronous machines like constant operation-speed, producing substantial savings by supplying reactive power to counteract lagging power factor caused by inductive loads, low inrush currents, and capabilities of designing the torque characteristics to meet the requirements of the driven load, have made them optimal options for a multitude of industries. Economical utilization of these machines and also increasing their efficiencies are issues that should receive significant attention.

At high power rating operations, where high switching efficiency in the drive circuits is of utmost importance, optimal pulsewidth modulation (PWM) is the logical feeding scheme (Holtz, 1992). Application of optimal PWM decreases overheating in machine and therefore results in diminution of torque pulsation. Overheating, resulted from internal losses, is a major factor in rating a machine. Moreover, setting up an appropriate cooling method is a particularly serious issue, increasing in intricacy with machine size. Among various approaches for achieving optimal PWM, *harmonic elimination method* is predominant ((Mohan et al., 1995), (Enjeti et al., 1990), (Sun et al., 1996), (Chiasson et al., 2004), (Czarkowski et al., 2002), (Sayyah et al., 2006c)). Since copper losses are fundamentally determined by current harmonics, defining a performance index related to undesirable effects of the harmonics is of the essence in lieu of focusing on specific harmonics (Bose, 2002). Herein, the total harmonic current distortion (THCD) is the objective function for minimization of machine losses.

Possessing asymmetrical structure in direct (d) and quadrature (q) axes makes a great difference in modeling of synchronous machines relative to induction ones. Particularly, it will be shown that the THCD in high-power synchronous machines is dependent upon some internal parameters of the machine; particularly l_q and l_d, the inductances of q and d axes, respectively. Based on gathered input and output data at a specific operating point, these parameters are determined using online identification methods (Ljung & Söderström, 1983). In light of the identified parameters, the problem is redrafted as an optimization task, and the optimal pulse patterns are sought through genetic algorithm (GA). Indeed, the complexity and nonlinearity of the proposed objective function increases the probability of trapping the

conventional optimization methods in suboptimal solutions. The GA provided with salient features [3]-[5], can cope effectively with shortcomings of the deterministic optimization methods.

The mentioned parameters are affected by several factors like modification in operating point, aging and temperature rise. Variations in these parameters invalidate the pre-calculated optimal pulse patterns and therefore impose excessive computational and processing burden; to carry out identification procedure, and subsequently optimization process to determine new optimal pulse patterns. Notwithstanding of accepting this computational burden and storing the accomplished optimal pulse patterns in read-only memories (ROMs) to serve as look-up tables (LUTs), substitution in LUTs provokes an adverse transient condition, which make it a formidable task (Rezazadeh et al., 2006).

In this study, optimal pulse patterns of induction machine (Sayyah et al., 2006b), whose total harmonic current distortion is independent of its parameters, as established in (Sun, 1995), are applied to current harmonic model of synchronous machines with different values of $\frac{l_q}{l_d}$. The results are compared with corresponding minimum power losses. Based on the demonstrated comparisons, if deviation from the minimum power losses is acceptable, application of optimal pulse patterns of induction machine (the so-called suboptimal solutions), is an appropriate alternative to preceding methods considering their excessive processing burdens.

2. Preliminaries and problem formulation

In this section, we examine the prerequisites for developing the approach of this study. Since the content has been set forth in preceding works (Rezazadeh et al., 2006), (Sayyah et al., 2006a), (Sayyah et al., 2006b), (Sayyah et al., 2006c), the discussions are provided for the sake of reproducibility.

2.1 Waveform representation

For the scope of this paper, a PWM waveform is a 2π-periodic function $f(\theta)$ with two distinct normalized levels of $-1, +1$ for $0 \leq t \leq \pi/2$ and has the symmetries $f(\theta) = f(\pi - \theta)$ and $f(\theta) = -f(2\pi - \theta)$.

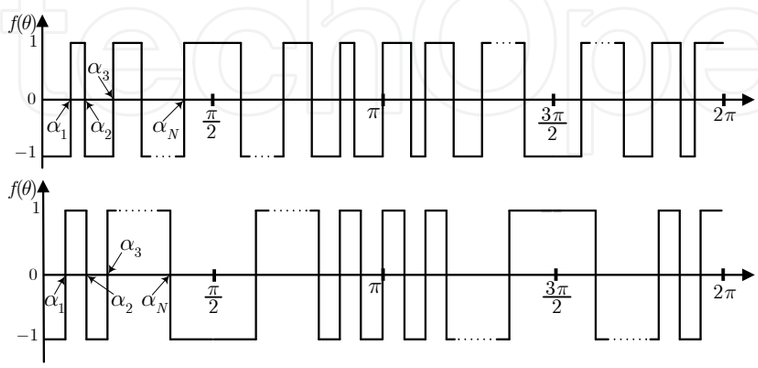

Fig. 1. A typical normalized PWM structure.

Owing to the symmetries in normalized PWM waveform of Fig. 1, only the odd harmonics exist. As such, $f(\theta)$ can be written with the Fourier series as

$$f(\theta) = \sum_{k=1,3,5,\ldots} u_k \sin(k\theta) \tag{1}$$

with

$$\begin{aligned} u_k &= \frac{4}{\pi}\int_0^{\frac{\pi}{2}} f(\theta)\sin(k\theta) \\ &= \frac{4}{k\pi}\big(-1+2\sum_{i=1}^{N}(-1)^{i-1}\cos(k\alpha_i)\big). \end{aligned} \tag{2}$$

2.2 THCD formulation in induction machine

The harmonic equivalent circuit and its approximation of an induction motor operating in steady-state conditions is illustrated in Fig. 2 (Sun, 1995).

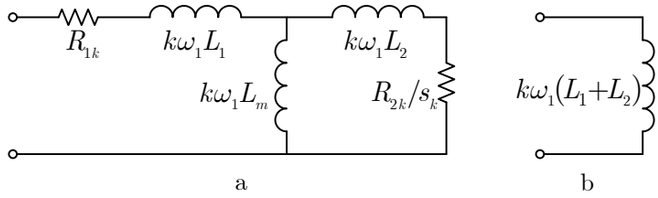

Fig. 2. Equivalent circuit of an induction motor operating in steady-state conditions: (a) The k^{th} order harmonic equivalent circuit, (b) Approximation of (a), $(k > 1)$.

The approximation of the equivalent circuit is deduced regarding the fact that inductive reactances increase linearly with frequency, while the stator and rotor resistances are almost constant. Since s_k is approximately unity, circuit resistance is negligible in comparison with reactance at the harmonic frequency. In addition, the magnetizing inductance L_m is much larger than the rotor leakage inductance L_2 and may be omitted. Hence, the motor impedance presented to the k^{th}-order harmonic input voltage is $k\omega_1(L_1 + L_2)$ and the k^{th}-order current harmonic would be:

$$I_k = \frac{u_k}{k\omega_1(L_1+L_2)} \propto \frac{u_k}{k}. \tag{3}$$

Thus, the objective function of this optimization can be stated as:

$$\sigma_i^{\text{ind}} = \sqrt{\sum_{k\in S_3}(u_k/k)^2}, \tag{4}$$

where $S_3 = \{5, 7, \ldots, 6l-1, 6l+1, \ldots\}$ stands for the set of triple harmonics in consideration.

Throughout the optimization procedure, it is desired to maintain the fundamental output voltage at a constant level: $V_1 = M$. M so-called the modulation index may be assumed to have any value between 0 and $\frac{4}{\pi}$. It can be shown that α_N is dependent on modulation index and the rest of $N-1$ switching angles. As such, one decision variable can be eliminated explicitly (Sayyah et al., 2006b).

2.3 THCD formulation in synchronous machine

In this section, we formulate the THCD in high-power synchronous machines. Some simplifications and assumptions are considered in modeling of these machines; space harmonics of the flux linkage distribution are neglected, linear magnetics due to operation in linear portion of magnetization curve prior to experiencing saturation knee is assumed, iron losses are neglected, and slot harmonics and deep bar effects are not considered.

Synchronous machine model equations can be written as follows (Holtz, 1995):

$$\boldsymbol{u}_S^R = \boldsymbol{r}_S \boldsymbol{i}_R^S + \jmath\omega \boldsymbol{\Psi}_S^R + \frac{d\boldsymbol{\Psi}_S^R}{d\tau}, \tag{5}$$

$$\mathbf{0} = \boldsymbol{R}_D \boldsymbol{i}_D + \frac{d\boldsymbol{\Psi}_D}{d\tau}, \tag{6}$$

$$\boldsymbol{\Psi}_S^R = \boldsymbol{l}_S \boldsymbol{i}_S^R + \boldsymbol{\Psi}_m^R, \tag{7}$$

$$\boldsymbol{\Psi}_m^R = \boldsymbol{l}_m (\boldsymbol{i}_D + \boldsymbol{i}_F), \tag{8}$$

$$\boldsymbol{\Psi}_D = \boldsymbol{l}_D \boldsymbol{i}_D + \boldsymbol{l}_m (\boldsymbol{i}_S + \boldsymbol{i}_F), \tag{9}$$

where:

$$\boldsymbol{l}_S = \boldsymbol{l}_{lS} + \boldsymbol{l}_m = \begin{pmatrix} l_d & 0 \\ 0 & l_q \end{pmatrix}, \quad \boldsymbol{i}_F = \begin{pmatrix} 1 \\ 0 \end{pmatrix} i_F, \tag{10}$$

and

$$\boldsymbol{l}_m = \begin{pmatrix} l_{md} & 0 \\ 0 & l_{mq} \end{pmatrix}, \quad \boldsymbol{l}_D = \begin{pmatrix} l_{Dd} & 0 \\ 0 & l_{Dq} \end{pmatrix}, \tag{11}$$

where l_d and l_q are inductances of the motor in d and q axes; $\boldsymbol{i}_D$ is damper winding current; $\boldsymbol{u}_S^R$ and $\boldsymbol{i}_S^R$ are stator voltage and current space vectors, respectively; $\boldsymbol{l}_D$ is the damper inductance; l_{md} is the d-axis magnetization inductance; l_{mq} is the q-axis magnetization inductance; l_{Dd} is the d-axis damper inductance; l_{Dq} is the q-axis damper inductance; $\boldsymbol{\Psi}_m$ is the magnetization flux; $\boldsymbol{\Psi}_D$ is the damper flux; i_F is the field excitation current and $\jmath \triangleq \sqrt{-1}$. Time is also normalized $\tau = \omega t$, where ω is the angular frequency. The total harmonic current distortion is defined as follows:

$$\sigma_i^{\text{synch}} = \sqrt{\frac{1}{T}\int_T [\boldsymbol{i}_S(t) - \boldsymbol{i}_{S1}(t)]^2 dt}, \tag{12}$$

in which $\boldsymbol{i}_{S1}$ is the fundamental component of stator current.

Assuming that the steady state operation of machine makes a constant exciting current, the dampers current in the system can be neglected. Therefore, we have the machine model in rotor coordinates as:

$$\boldsymbol{u}_S^R = \boldsymbol{r}_S \boldsymbol{i}_S^R + \jmath\omega \boldsymbol{l}_S \boldsymbol{i}_S^R + \jmath\omega \boldsymbol{l}_m \boldsymbol{i}_F + \boldsymbol{l}_S \frac{d\boldsymbol{i}_S^R}{d\tau}. \tag{13}$$

With the *Park* transformation, we have the machine model in stator coordinates (the so-called $\alpha - \beta$ coordinates) as:

$$\begin{aligned} \boldsymbol{u}_{\alpha\beta} = {} & R_S \boldsymbol{i}_{\alpha\beta} + \omega(l_d - l_q) \begin{pmatrix} -\sin 2\theta & \cos 2\theta \\ \cos 2\theta & \sin 2\theta \end{pmatrix} \boldsymbol{i}_{\alpha\beta} + \frac{l_d - l_q}{2} \begin{pmatrix} \cos 2\theta & \sin 2\theta \\ \sin 2\theta & -\cos 2\theta \end{pmatrix} \frac{d\boldsymbol{i}_{\alpha\beta}}{d\tau} \\ & + \frac{l_d + l_q}{2} \frac{d\boldsymbol{i}_{\alpha\beta}}{d\tau} + \omega l_{md} \begin{pmatrix} -\sin\theta \\ \cos\theta \end{pmatrix} i_F, \end{aligned} \tag{14}$$

in which θ is the rotor angle. Neglecting the ohmic terms in (14), we have:

$$\boldsymbol{u}_{\alpha\beta} = \frac{d}{d\tau}(\boldsymbol{l}_S(\theta)\boldsymbol{i}_{\alpha\beta}) + l_{md}\frac{d}{d\tau}\Big(\begin{pmatrix}\cos\theta\\ \sin\theta\end{pmatrix} i_F\Big), \tag{15}$$

in which:

$$\boldsymbol{l}_S(\theta) = \frac{l_d + l_q}{2}\mathbf{I}_2 + \frac{l_d - l_q}{2}\begin{pmatrix}\cos 2\theta & \sin 2\theta\\ \sin 2\theta & -\cos 2\theta\end{pmatrix}. \tag{16}$$

$\mathbf{I}_2$ is the 2×2 identity matrix. Hence:

$$\begin{aligned}\boldsymbol{i}_{\alpha\beta} &= \boldsymbol{l}_S^{-1}(\theta)\cdot\Big(\int \boldsymbol{u}_{\alpha\beta}d\tau - l_{md}\begin{pmatrix}\cos\theta\\ \sin\theta\end{pmatrix} i_F\Big)\\ &= \begin{pmatrix}\frac{l_d+l_q}{2l_dl_q} - \frac{l_d-l_q}{2l_dl_q}\cos 2\theta & -\frac{l_d-l_q}{2l_dl_q}\sin 2\theta\\ -\frac{l_d-l_q}{2l_dl_q}\sin 2\theta & \frac{l_d+l_q}{2l_dl_q} + \frac{l_d-l_q}{2l_dl_q}\cos 2\theta\end{pmatrix}\cdot\Big\{\int \boldsymbol{u}_{\alpha\beta}d\tau - l_{md}\begin{pmatrix}\cos\theta\\ \sin\theta\end{pmatrix} i_F\Big\}\\ &= \Big(\frac{l_d + l_q}{2l_dl_q}\mathbf{I}_2 - \frac{l_d - l_q}{2l_dl_q}\begin{pmatrix}\cos 2\theta & \sin 2\theta\\ \sin 2\theta & -\cos 2\theta\end{pmatrix}\Big)\cdot\Big(\int \boldsymbol{u}_{\alpha\beta}d\tau - l_{md}\begin{pmatrix}\cos\theta\\ \sin\theta\end{pmatrix} i_F\Big).\end{aligned} \tag{17}$$

With further simplification, we have $\boldsymbol{i}_{\alpha\beta}$ as:

$$\boldsymbol{i}_{\alpha\beta} = \frac{l_d + l_q}{2l_dl_q}\int \boldsymbol{u}_{\alpha\beta}d\tau + J_1 - \frac{l_d - l_q}{2l_dl_q}J_2, \tag{18}$$

in which:

$$J_1 = -l_{md}\frac{l_d + l_q}{2l_dl_q}\begin{pmatrix}\cos\theta\\ \sin\theta\end{pmatrix} i_F + l_{md}\frac{l_d - l_q}{2l_dl_q}\begin{pmatrix}\cos 2\theta & \sin 2\theta\\ \sin 2\theta & -\cos 2\theta\end{pmatrix}\cdot\begin{pmatrix}\cos\theta\\ \sin\theta\end{pmatrix}, \tag{19}$$

and

$$J_2 = \begin{pmatrix}\cos 2\theta & \sin 2\theta\\ \sin 2\theta & -\cos 2\theta\end{pmatrix}\cdot\int \boldsymbol{u}_{\alpha\beta}d\tau. \tag{20}$$

Using the trigonometric identities, $\cos(\theta_1 - \theta_2) = \cos\theta_1\cos\theta_2 + \sin\theta_1\sin\theta_2$ and $\sin(\theta_1 - \theta_2) = \sin\theta_1\cos\theta_2 - \cos\theta_1\sin\theta_2$, the term J_1 in Equation 18 can be simplified as:

$$\begin{aligned}J_1 &= -l_{md}\frac{l_d + l_q}{2l_dl_q}\begin{pmatrix}\cos\theta\\ \sin\theta\end{pmatrix} i_F + l_{md}\frac{l_d - l_q}{2l_dl_q}\begin{pmatrix}\cos 2\theta\cdot\cos\theta + \sin 2\theta\cdot\sin\theta\\ \sin 2\theta\cdot\cos\theta - \cos 2\theta\cdot\cos\theta\end{pmatrix} i_F\\ &= -l_{md}\frac{l_d + l_q}{2l_dl_q}\begin{pmatrix}\cos\theta\\ \sin\theta\end{pmatrix} i_F + l_{md}\frac{l_d - l_q}{2l_dl_q}\begin{pmatrix}\cos\theta\\ \sin\theta\end{pmatrix} i_F\\ &= \frac{l_{md}}{l_d}\begin{pmatrix}\cos\theta\\ \sin\theta\end{pmatrix} i_F.\end{aligned} \tag{21}$$

On the other hand, writing the phase voltages in Fourier series:

$$u_A = \sum_{s\in S_3} u_{2s+1}\sin((2s+1)\theta),$$
$$u_B = \sum_{s\in S_3} u_{2s+1}\sin((2s+1)(\theta-\frac{2\pi}{3})),$$
$$u_C = \sum_{s\in S_3} u_{2s+1}\sin((2s+1)(\theta-\frac{4\pi}{3})),$$

and using 3-phase to 2-phase transformation, we have:

$$\begin{pmatrix} u_\alpha \\ u_\beta \end{pmatrix} = \begin{pmatrix} u_A \\ \frac{1}{\sqrt{3}}(u_B-u_C) \end{pmatrix} = \begin{pmatrix} \sum_{s\in S_3} u_s\sin(s\theta) \\ \sum_{s\in S_3} u_s\sin(s(\theta-\frac{2\pi}{3})+\varphi_s) \end{pmatrix} \tag{22}$$

in which:

$$\varphi_s = \begin{cases} \frac{\pi}{6} & \text{for } s=1,7,13,\cdots \\ -\frac{\pi}{6} & \text{for } s=5,11,17,\cdots \end{cases}.$$

As such, we have:

$$\boldsymbol{u}_{\alpha\beta} = \begin{pmatrix} \sum_{l=0}^{\infty} u_{6l+1}\sin((6l+1)\theta) \\ \sum_{l=0}^{\infty} u_{6l+1}\sin((6l+1)(\theta-\frac{2\pi}{3})+\frac{\pi}{6}) \end{pmatrix} + \begin{pmatrix} \sum_{l=0}^{\infty} u_{6l+5}\sin((6l+5)\theta) \\ \sum_{l=0}^{\infty} u_{6l+5}\sin((6l+5)(\theta-\frac{2\pi}{3})-\frac{\pi}{6}) \end{pmatrix}. \tag{23}$$

Integration of $\boldsymbol{u}_{\alpha\beta}$ yields:

$$\begin{aligned} \int \boldsymbol{u}_{\alpha\beta}d\tau &= -\frac{1}{\omega}\times \\ &\left\{ \begin{pmatrix} \sum_{l=0}^{\infty}\frac{u_{6l+1}}{6l+1}\cos((6l+1)\theta) \\ \sum_{l=0}^{\infty}\frac{u_{6l+1}}{6l+1}\cos((6l+1)\theta-4\pi l-\frac{\pi}{2}) \end{pmatrix} \right. \\ &\left. + \begin{pmatrix} \sum_{l=0}^{\infty}\frac{u_{6l+5}}{6l+5}\cos((6l+5)\theta) \\ \sum_{l=0}^{\infty}\frac{u_{6l+5}}{6l+5}\cos((6l+5)\theta-4\pi l-\frac{3\pi}{2}) \end{pmatrix} \right\} \\ &= -\frac{1}{\omega}\times \begin{pmatrix} \sum_{l=0}^{\infty}[\frac{u_{6l+1}}{6l+1}\cos((6l+1)\theta)+\frac{u_{6l+5}}{6l+5}\cos((6l+5)\theta)] \\ \sum_{l=0}^{\infty}[\frac{u_{6l+1}}{6l+1}\sin((6l+1)\theta)-\frac{u_{6l+5}}{6l+5}\sin((6l+5)\theta)] \end{pmatrix} \end{aligned} \tag{24}$$

By substitution of $\int \boldsymbol{u}_{\alpha\beta}d\tau$ in Equation 18, the term J_2 can be written as:

$$\begin{aligned} J_2 &= \begin{pmatrix} \cos 2\theta & \sin 2\theta \\ \sin 2\theta & -\cos 2\theta \end{pmatrix}\cdot\int \boldsymbol{u}_{\alpha\beta}d\tau = -\frac{1}{\omega}\times \\ &\left\{ \begin{pmatrix} \sum_{l=0}^{\infty}\frac{u_{6l+1}}{6l+1}\cos((6l+1)\theta)\cdot\cos 2\theta \\ \sum_{l=0}^{\infty}\frac{u_{6l+1}}{6l+1}\cos((6l+1)\theta)\cdot\sin 2\theta \end{pmatrix} + \begin{pmatrix} \sum_{l=0}^{\infty}\frac{u_{6l+1}}{6l+1}\sin((6l+1)\theta)\cdot\sin 2\theta \\ -\sum_{l=0}^{\infty}\frac{u_{6l+1}}{6l+1}\sin((6l+1)\theta)\cdot\cos 2\theta \end{pmatrix} \right. \\ &\left. + \begin{pmatrix} \sum_{l=0}^{\infty}\frac{u_{6l+5}}{6l+5}\cos((6l+5)\theta)\cdot\cos 2\theta \\ \sum_{l=0}^{\infty}\frac{u_{6l+5}}{6l+5}\cos((6l+5)\theta)\cdot\sin 2\theta \end{pmatrix} + \begin{pmatrix} -\sum_{l=0}^{\infty}\frac{u_{6l+5}}{6l+5}\sin((6l+5)\theta)\cdot\sin 2\theta \\ \sum_{l=0}^{\infty}\frac{u_{6l+5}}{6l+5}\sin((6l+5)\theta)\cdot\cos 2\theta \end{pmatrix} \right\} \\ &= -\frac{1}{\omega}\begin{pmatrix} \sum_{l=0}^{\infty}[\frac{u_{6l+1}}{6l+1}\cos((6l-1)\theta)+\frac{u_{6l+5}}{6l+5}\cos((6l+7)\theta)] \\ \sum_{l=0}^{\infty}[-\frac{u_{6l+1}}{6l+1}\sin((6l-1)\theta)+\frac{u_{6l+5}}{6l+5}\sin((6l+7)\theta)] \end{pmatrix}. \end{aligned} \tag{25}$$

Considering the derived results, we can rewrite $i_A = i_\alpha$ as:

$$i_A = \Big(-\frac{l_d + l_q}{2l_d l_q \omega}\Big) \cdot \sum_{l=0}^{\infty} [\frac{u_{6l+1}}{6l+1} \cos((6l+1)\theta) + \frac{u_{6l+5}}{6l+5} \cos((6l+5)\theta)]$$
$$+ \Big(\frac{l_d - l_q}{2l_d l_q \omega}\Big) \cdot \sum_{l=0}^{\infty} [\frac{u_{6l+1}}{6l+1} \cos((6l-1)\theta) + \frac{u_{6l+5}}{6l+5} \cos((6l+7)\theta)] - \frac{l_{md}}{l_d} i_F \cos\theta. \quad (26)$$

Using the appropriate dummy variables $l = l' + 1$ and $l = l'' - 1$, we have:

$$\begin{aligned} i_A &= \Big(-\frac{l_d + l_q}{2l_d l_q \omega}\Big) \cdot \Big\{ \sum_{l=0}^{\infty} \frac{u_{6l+1}}{6l+1} \cos((6l+1)\theta) + \sum_{l=0}^{\infty} \frac{u_{6l+5}}{6l+5} \cos((6l+5)\theta) \Big\} + \\ &\Big(\frac{l_d - l_q}{2l_d l_q \omega}\Big) \cdot \Big\{ \sum_{l'=-1}^{\infty} \frac{u_{6l'+7}}{6l'+7} \cos((6l'+5)\theta) + \sum_{l''=1}^{\infty} \frac{u_{6l''-1}}{6l''-1} \cos((6l''+1)\theta) \Big\} \\ &- \frac{l_{md}}{l_d} i_F \cos\theta \\ &= \Big(-\frac{l_d + l_q}{2l_d l_q \omega}\Big) \cdot \Big\{ \sum_{l=0}^{\infty} \frac{u_{6l+1}}{6l+1} \cos((6l+1)\theta) + \sum_{l=0}^{\infty} \frac{u_{6l+5}}{6l+5} \cos((6l+5)\theta) \Big\} \\ &+ \Big(\frac{l_d - l_q}{2l_d l_q \omega}\Big) \cdot \Big\{ \sum_{l=0}^{\infty} \frac{u_{6l+7}}{6l+7} \cos((6l+5)\theta) + \sum_{l=0}^{\infty} \frac{u_{6l-1}}{6l-1} \cos((6l+1)\theta) + u_1 \cos\theta \Big\} \\ &- \frac{l_{md}}{l_d} i_F \cos\theta. \end{aligned} \quad (27)$$

Thus, we have i_A as:

$$\begin{aligned} i_A \; &= \Big(-\frac{1}{2l_d l_q \omega}\Big) \cdot \Big\{ \sum_{l=0}^{\infty} [(l_d + l_q)\frac{u_{6l+1}}{6l+1} - (l_d - l_q)\frac{u_{6l-1}}{6l-1}] \cdot \cos((6l+1)\theta) + \\ &\sum_{l=0}^{\infty} [(l_d + l_q)\frac{u_{6l+5}}{6l+5} - (l_d - l_q)\frac{u_{6l+7}}{6l+7}] \cdot \cos((6l+1)\theta) - (l_d - l_q) u_1 \cos\theta \Big\} \\ &- \frac{l_{md}}{l_d} i_F \cos\theta. \end{aligned} \quad (28)$$

Removing the fundamental components from Equation 28, we have:

$$\begin{aligned} i_{Ah} &= \Big(-\frac{1}{2l_d l_q \omega}\Big) \cdot \Big\{ \sum_{l=1}^{\infty} \big[\big\{ (l_d + l_q)\frac{u_{6l+1}}{6l+1} - (l_d - l_q)\frac{u_{6l-1}}{6l-1} \big\} \cdot \cos((6l+1)\theta) \big] + \\ &\sum_{l=0}^{\infty} \big[\big\{ (l_d + l_q)\frac{u_{6l+5}}{6l+5} - (l_d - l_q)\frac{u_{6l+7}}{6l+7} \big\} \cdot \cos((6l+5)\theta) \big] \Big\} \\ &= \Big(-\frac{1}{2l_d l_q \omega}\Big) \cdot \Big\{ \sum_{l=0}^{\infty} \big\{ (l_d + l_q)\frac{u_{6l+7}}{6l+7} - (l_d - l_q)\frac{u_{6l+5}}{6l+5} \big\} \cdot \cos((6l+7)\theta) + \\ &\sum_{l=0}^{\infty} \big\{ (l_d + l_q)\frac{u_{6l+5}}{6l+5} - (l_d - l_q)\frac{u_{6l+7}}{6l+7} \big\} \cdot \cos((6l+5)\theta) \Big\}. \end{aligned} \quad (29)$$

On the other hand, σ_l^2 can be written as:

$$\begin{aligned}\sigma_l^2 &= \Big((l_d+l_q)\frac{u_{6l+7}}{6l+7}-(l_d-l_q)\frac{u_{6l+5}}{6l+5}\Big)^2+\Big((l_d+l_q)\frac{u_{6l+5}}{6l+5}-(l_d-l_q)\frac{u_{6l+7}}{6l+7}\Big)^2\\ &= 2(l_d^2+l_q^2)\Big(\frac{u_{6l+7}}{6l+7}\Big)^2+2(l_d^2+l_q^2)\Big(\frac{u_{6l+5}}{6l+5}\Big)^2-4(l_d^2-l_q^2)\frac{u_{6l+5}u_{6l+7}}{(6l+5)(6l+7)}.\end{aligned} \tag{30}$$

With normalization of σ_l^2; i.e. $\tilde{\sigma}_l^2=\frac{\sigma_l^2}{l_d^2+l_q^2}$ and also the definition of the total harmonic current distortion as $\sigma_i^2=\sum_{l=0}^{\infty}\tilde{\sigma}_l^2$, we have:

$$\sigma_i^2=\sum_{l=0}^{\infty}\Big\{\Big(\frac{u_{6l+5}}{6l+5}\Big)^2+\Big(\frac{u_{6l+7}}{6l+7}\Big)^2-2\frac{l_d^2-l_q^2}{l_d^2+l_q^2}\Big(\frac{u_{6l+5}}{6l+5}\Big)\Big(\frac{u_{6l+7}}{6l+7}\Big)\Big\}.$$

Considering the set $S_3=\{5,7,11,13,\cdots\}$ and with more simplification, σ_i in high-power synchronous machines can be explicitly expressed as:

$$\sigma_i=\sqrt{\sum_{k\in S_3}\Big(\frac{u_k}{k}\Big)^2-2\frac{l_d^2-l_q^2}{l_d^2+l_q^2}\sum_{l=1}^{\infty}\Big(\frac{u_{6l-1}}{6l-1}\Big)\cdot\Big(\frac{u_{6l+1}}{6l+1}\Big)}. \tag{31}$$

As mentioned earlier, THCD in high-power synchronous machines depends on l_d and l_q, the inductances of d and q axes, respectively.

3. Switching scheme

Switching frequency in high-power systems, due to the use of gate turn-off thyristor (GTO) in the inverter is limited to several hundred hertz. In this work, the switching frequency has been set to $f_s=200$ Hz. Considering the frequency of the fundamental component of PWM waveform to be variable with maximum value of 50 Hz (i.e. $f_{1\max}=50$ Hz), we have: $\frac{f_s}{f_{1\max}}=4$. This condition forces a constraint on the number of switches, since we have:

$$\frac{f_s}{f_1}=N. \tag{32}$$

On the other hand, in electrical machines with rotating magnetic field, in order to maintain the torque at a constant level, the fundamental frequency of the PWM should be proportional to its amplitude (modulation index is also proportional to the amplitude) (Leonhard, 2001). That is:

$$M=kf_1=\frac{k}{N}\cdot f_s=k\cdot\frac{f_{1\max}}{N}\cdot\frac{f_s}{f_{1\max}}. \tag{33}$$

Also, we have:

$$M=kf_1|_{f_1=f_{1\max}}=1\Rightarrow k=\frac{1}{f_{1\max}}. \tag{34}$$

Considering Equations (33) and (34), the following equation is resulted:

$$\frac{f_s}{f_{1\max}}=M\cdot N. \tag{35}$$

The value of $\frac{f_s}{f_{1\max}}$ is plotted versus modulation index in Figure 3.

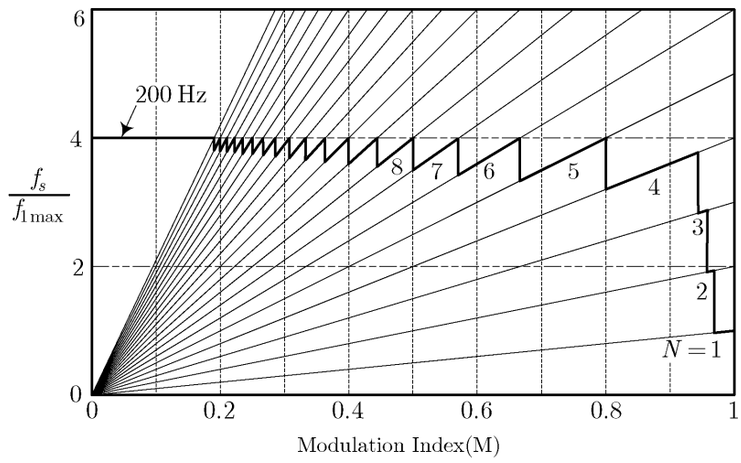

Fig. 3. Switching scheme

Figure 3 shows that as the number of switching angles increases and M declines from unity, the curve moves towards the upper limit $\frac{f_s}{f_{1\max}}$. The curve, however, always remains under the upper limit. When N increases and reaches a large amount, optimization procedure and its accomplished results are not effective. Additionally, it does not show a significant advantage in comparison with space vector PWM (SVPWM). Based on this fact, in high power machines, the feeding scheme is a combination of optimized PWM and SVPWM.

At this juncture, feedforward structure of PWM fed inverter is emphasized. Presence of current feedback path means that the switching frequency is dictated by the current which is the follow-on of system dynamics and load conditions. This may give rise to uncontrollable high switching frequencies that indubitably denote colossal losses. Furthermore, utilization of current feedback for PWM generation intensifies system instability and results in chaos.

4. Optimization procedure

A numerical optimization algorithm is expected to perform the task of global optimization of an objective function. However, as objective function may possess numerous local optima, algorithms are prone to get trapped in local solutions. The genetic algorithms (GAs) among the numerical algorithms, have been extensively used as search and optimization tools in dealing with global optimization problems, due to their capability of avoiding local solutions from terminating the optimization process. There are certain other advantages to GAs such as their indifference to system specific information, especially the derivative information, the versatility of application, the ease with which heuristics can be incorporated in optimization, the capability of learning and adapting to changes over time, the implicitly parallel directed random exploration of the search space, and the ability to accommodate discrete variables in the search process, to name a few (Bäck et al., 1997).

GAs operate on a population of potential solutions to generate close approximations to the optimal solution through evolution. The population is a set of chromosomes, and the basic GA operators are selection, crossover and mutation. At each generation, a new set

of approximations is created by the process of selecting individuals and breeding them together using crossover and mutation operators which are conceptually borrowed from natural genetics. This process leads to the evolution of better individuals with near-optimum solutions over time.

The GA methodology structure for the problem considered herein is as follows:

1. Feasible individuals are generated randomly for initial population. That is a $n \times (N-1)$ random matrix, in which the rows' elements are sorted in ascending order, lying in $[0, \frac{\pi}{2}]$ interval.
2. Objective-function-value of all members of the population is evaluated by σ_i. This allows estimation of the probability of each individual to be selected for reproduction.
3. Selection of individuals for reproduction is done. When selection of individuals for reproduction is done, crossover and mutation are applied, based on forthcoming arguments. New population is created and this procedure continues from step (2). This procedure is repeated until a termination criterion is reached.

Whether the algorithm will find a near-optimum solution and whether it will find such a solution efficiently is determined through proper choosing of GA parameters. In the sequel, some arguments for strategies in setting the components of GA can be found.

Population size plays a pivotal role in the performance of the algorithm. Large sizes of population decrease the speed of convergence, but help maintain the population diversity and therefore reduce the probability for the algorithm to trap into local optima. Small population sizes, on the contrary, may lead to premature convergences. With choosing the population size as $\lfloor (10 \cdot N)^{1.2} \rfloor$, in which the bracket $\lfloor \cdot \rfloor$ marks that the integer part is taken, satisfying results are yielded.

Gaussian mutation step size (Eiben et al., 1999) is used with arithmetical crossover to produce offspring for the next generation. Mutations are realized by replacing components of the vector $\boldsymbol{\alpha}$ by

$$\alpha_i' = \alpha_i + \mathcal{N}(0, \sigma) \tag{36}$$

where $\mathcal{N}(0, \sigma)$ is a random Gaussian number with mean zero and standard deviation σ. We replaced the static parameter σ by a dynamic parameter, a function $\sigma(t)$ defined as

$$\sigma(t) = 1 - \frac{t}{T} \tag{37}$$

where t is the current generation number varying from zero to T, which is the maximum generation number.

Here, the mutation step size $\sigma(t)$ will decrease slowly from one at the beginning of the run $(t = 0)$ to 0 as the number of generations t approaches T. We set the mutation probability (P_m) to a fixed value of 0.2 throughout all stages of optimization process. One purpose of having a relatively high mutation rate is to maintain the population diversity, explore the search space effectively and prevent premature convergence. Arithmetical crossover (Michalewicz, 1996) is considered herein, and probability of this operator is set to 0.8. When two parent individuals are denoted as $\boldsymbol{\alpha}^k = (\alpha_1^k, \ldots, \alpha_M^k), k \in \{1, 2\}$, two offspring $\boldsymbol{\alpha}'^k = (\alpha_1'^k, \ldots, \alpha_M'^k)$ are reproduced

as interpolations of both parents' genes:

$$\alpha_m'^1 = \lambda\alpha_m^1 + (1-\lambda)\alpha_m^2$$
$$\alpha_m'^2 = (1-\lambda)\alpha_m^1 + \lambda\alpha_m^2 \quad (38)$$

where the parameter λ, is a randomly chosen number in the interval [0,1].

There are different selection methods that can be used in the GAs algorithm. Tournament selection (Goldberg, 1989) with size 2 is one of these methods which is used as the selection mechanism in this study. An elitist strategy is also enabled during the replacement operation. Elitism usually brings about a more rapid convergence of the population and also improves the chances of locating the optimal individual. Elite count considered in this study is 5% of population size. In this study the termination criteria is reaching 500^{th} generation, which stated that the algorithm is repeated until a predetermined number of generations is reached. It should be noted that to increase the precision of the optimal solutions accomplished by the algorithm, we used a local search function which finds the minimum of a scalar function of several variables, starting at initial estimate which is the outcome of the GA.

5. Optimal pulse patterns for synchronous machines

The characteristics of electric machines depend decisively upon the use of magnetic materials. These materials are required to form the magnetic circuit and are used by the machine designers to obtain specific desired characteristics. Striving to attain optimal usage of magnetic material, and consequently reduce its dimensions, volume and cost, has concentrated endeavors in the design of electric machines on locating machine's rated operating point near the saturation knee of magnetization curve. Furthermore, modifications in operating point, probably caused by various factors, results in substantial changes in machine's inductances. Considering the disproportion between the air gaps in d- and q-axis (q-axis air gap is larger), d-axis inductance experiences saturation region more quickly. This appreciably influences the value of $\frac{l_q}{l_d}$. Other factors, namely aging and temperature rise should also be taken into account in studying the variations of machine's inductances.

Based on discussion above, online identification of machine's inductances seems indispensable. Either an optimization procedure is to be performed or pre-determined $\frac{l_q}{l_d}$s are to be used for addressing the corresponding LUT and switching patterns to control the inverter. The latter is possible only in case various LUTs are available for different values of $\frac{l_q}{l_d}$.

Regarding identification algorithms for synchronous machines, unavailability of numerous machine variables, like dampers current, leads to negligence of such dynamics. As a result, bias in identified parameters, and deviation from their real values are quite possible. Considering the sensitivity of the problem to $\frac{l_q}{l_d}$, presence of bias in these parameters leads to arriving at switching patterns that are different from optimal ones. As observed, online identification procedure and offline calculation of optimal pulse patterns, both, require immoderate processing burden. Substitution in LUTs, causes transient conditions. The drawbacks associated with transient conditions can briefly be stated as follows:

1. Power losses increase during transition and reduction in THCD is not realized.

2. Intensification of transient conditions may reach an unacceptable level and cause system to trip.

Hence, considerable efforts to compensate transient conditions, while keeping system's operating point fixed, enhance system's cost.

6. Comparison results

Accomplished optimal pulse patterns for induction motor, which are the fundamental components for the performed comparison, are shown in Fig. 4.

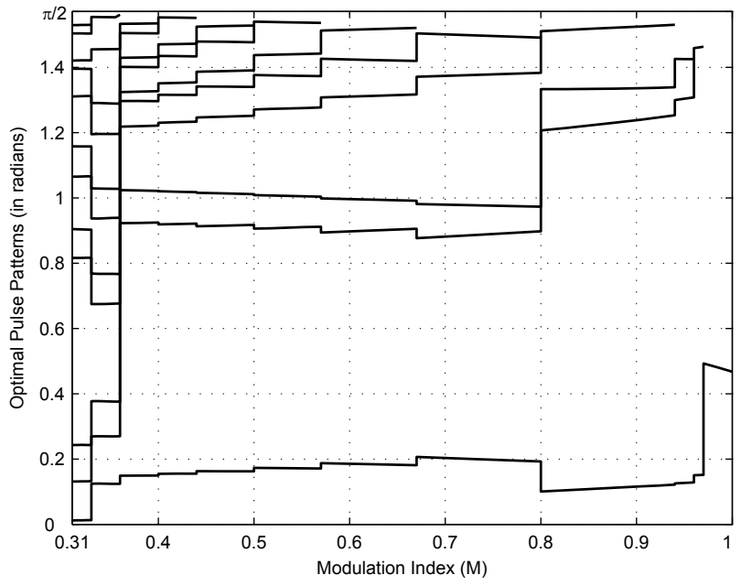

Fig. 4. Optimal pulse patterns of induction motor.

To distinguish between suboptimal and global solutions, the insight on the distribution scheme of switching angles over the considered interval (i.e. $[0, \frac{\pi}{2}]$), along with tracing the increase in the number of switching angles, were of significant assistances. Also, optimal pulse patterns in synchronous machines for $\frac{l_q}{l_d} = 0.3$ are shown in Fig. 5.

Minimized THCD and resulted THCD using optimal pulse patterns of induction motor (suboptimal solutions) are illustrated in Fig. 6 for $\frac{l_q}{l_d} = 0.3$.

For comparison, an index is defined:

$$\text{Error Percentage} = \frac{\sigma_i^{\text{synch}*} - \sigma_i^{\text{synch}}}{\sigma_i^{\text{synch}}} \times 100\%, \tag{39}$$

in which $\sigma_i^{\text{synch}*}$ denotes the resulted THCD of synchronous machines using optimal switches of induction motor. For $\frac{l_q}{l_d} = 0.3$ to 0.8 with increments of 0.1, the Error Percentages are illustrated in Fig. 7. Since the resulted system is intended for use in high modulation indices, the proposed approach is quite justifiable, considering these comparison results.

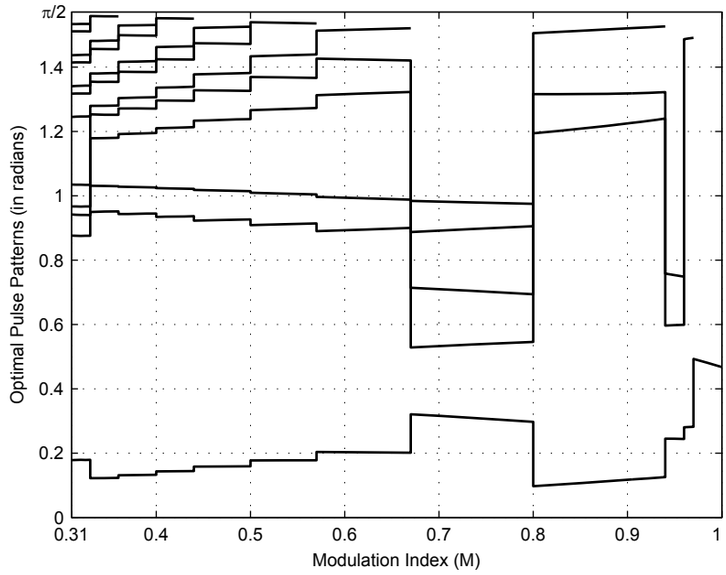

Fig. 5. Optimal pulse patterns of synchronous machine for $\frac{l_q}{l_d} = 0.3$.

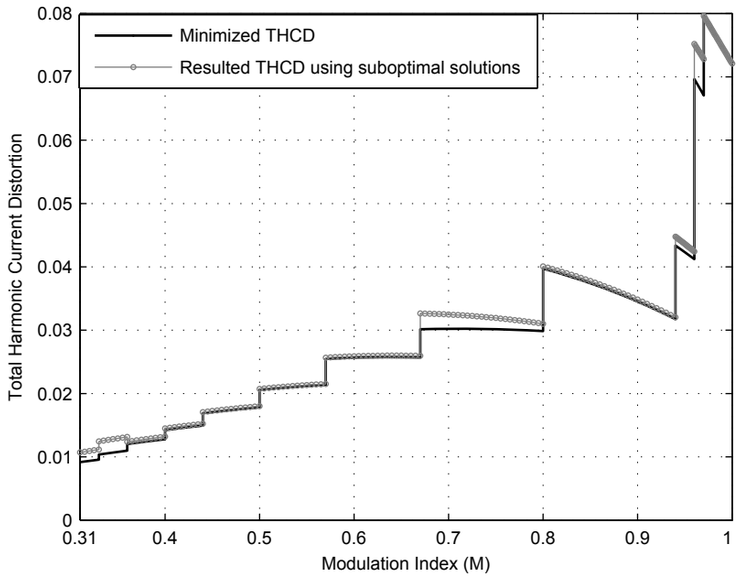

Fig. 6. Comparison between minimized THCD and resulted THCD in synchronous machine using suboptimal solutions for $\frac{l_q}{l_d} = 0.3$.

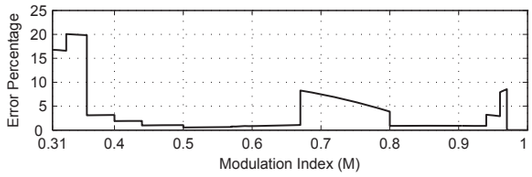

(a) $\frac{l_q}{l_d} = 0.3$

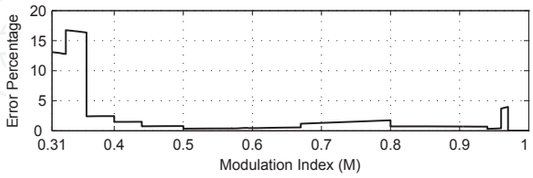

(b) $\frac{l_q}{l_d} = 0.4$

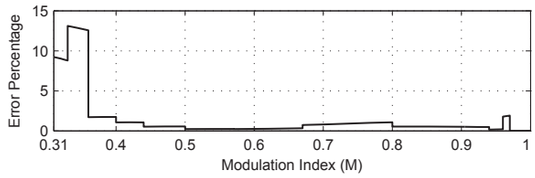

(c) $\frac{l_q}{l_d} = 0.5$

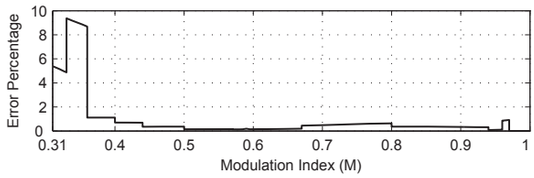

(d) $\frac{l_q}{l_d} = 0.6$

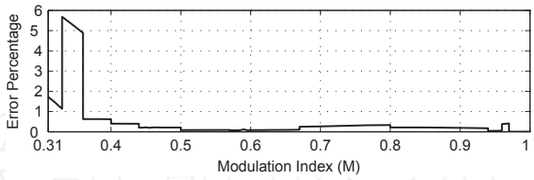

(e) $\frac{l_q}{l_d} = 0.7$

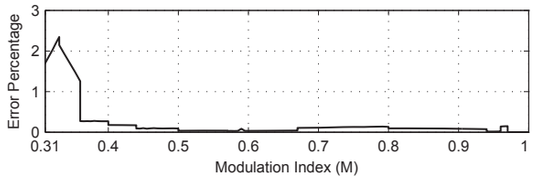

(f) $\frac{l_q}{l_d} = 0.8$

Fig. 7. Comparison results for distinct values of $\frac{l_q}{l_d}$.

7. Conclusions

This paper presents an efficient alternative approach for minimization of harmonic losses in high-power synchronous machines. The proposed current harmonic model in these machines is dependent on the inductances of d and q axes, the inductances in direct and quadrature axes, respectively. As high power application is of concern, finding the global optimum solution to have minimum losses in every specific operating point is of great consequence. For an identified typical machine, with specified characteristics, the problem is redrafted as an optimization task, and the optimal pulse patterns are sought through genetic algorithm (GA) in order to minimize the total harmonic current distortion (THCD). Optimal pulsewidth modulation (PWM) waveforms are accomplished up to 12 switches (per quarter period of PWM waveform), in which for more than this number of switching angles, space vector PWM (SVPWM) method, is preferred to optimal PWM approach. Selection of GA as the optimization method seems completely defensible considering its salient features which can cope with shortcomings of the deterministic optimization methods, particularly when decision variables increase, more probability of finding the global optimum solution, and also nonlinearity and complexity of the proposed objective function.

The aforementioned inductances are appreciably influenced by modifications in operating point, aging, and temperature rise. As such, in-progress switching patterns are no longer global optimum patterns, therefore performing optimization process to determine new optimal pulse patterns from among prior identification procedure results, is indispensable. Substitution in switching patterns provokes an unfavorable transient condition. Optimal pulse patterns of induction motor, whose current harmonic model is independent of its parameters, are applied to harmonic model of synchronous machine with distinct values of $\frac{l_q}{l_d}$. Effectiveness of the proposed approach is noteworthy, particularly in large values of $\frac{l_q}{l_d}$ and high modulation indices.

8. Acknowledgments

The authors would like to thank Professor Joachim Holtz of the University of Wuppertal for apposite suggestion of the approach developed in this study.

9. References

Bäck, T.; Hammel, U. & Schwefel, H. P. (1997). Evolutionary computation: comments on the history and current state. *IEEE Transactions on Evolutionary Computation*, Vol. 1, No. 1, April 1997, 3-17.

Boldea, I. & Nasar, S. A. (1992). *Vector Control of AC Drives*, CRC Press, Boca Raton, FL.

Bose, B. K. (2002). *Modern Power Electronics and AC Drives*, Prentice Hall, Upper Saddle River, NJ.

Chiasson, J.; Tolbert, L. M.; McKenzie, K. & Du, Z.: (2004). A complete solution to the harmonic elimination problem. *IEEE Transactions on Power Electronics*, Vol. 19, No. 2, March 2004, 491-499.

Czarkowski, D.; Chudnovsky, D. V.; Chudnovsky, G. V. & Selesnick, I. W. (2002). Solving the optimal PWM problem for single-phase inverters. *IEEE Transactions on Circuits and Systems–I*, Vol. 49, No. 4, April 2002, 465-475.

Davis, L. (1991). *Handbook of genetic algorithms*, Van Nostrand Reinhold, New York.

Eiben, *Á*. E.; Hinterding, R. & Michalewicz, Z. (1999). Parameter control in evolutionary algorithms. *IEEE Transactions on Evolutionary Computation*, Vol. 3, No. 2, July 1999, 124-141.

Enjeti, P. N. ; Ziogas, P. D. & Lindsay J. F. (1990). Programmed PWM techniques to eliminate harmonics: a critical evaluation. *IEEE Transactions on Industrial Applications*, Vol. 26, No. 2, Mar./Apr. 1990, 302âĂŞ316.

Goldberg, D. E. (1989). *Genetic algorithms in search, optimization and machine learning*, Addison-Wesley, Reading, MA.

Holtz, J. (1992). Pulsewidth modulation–a survey. *IEEE Transactions on Industrial Electronics*, Vol. 39, No. 5, December 1992, 410-419.

Holtz, J. (1995). The representation of ac machine dynamics by complex signal flow graphs. *IEEE Transactions on Industrial Electronics*, Vol. 42, No. 3, June 1995, 263-271

Leonhard, W. (2001). *Control of Electrical Erives*, 3rd ed., Springer-Verlag, New York.

Ljung, L. & Söderström, T. (1983). *Theory and Practice of Recursive Identification*, MIT Press, Cambridge, MA.

Michalewicz, Z. (1996). *Genetic algorithms + data structures=evolution programs*, Springer-Verlag, New York.

Mohan, N.; Undeland, T. M. & Robbins, W. P. (1995). *Power electronics: converters, applications, and design*, Wiley, New York.

Rezazadeh, A. R.; Sayyah, A. & Aflaki, M. (2006). Modulation error observation and regulation for use in off-line optimal PWM fed high power synchronous motors, *Proceedings of 1st IEEE conference on industrial electronics and applications*, pp. 1300-1307, May 2006, Singapore

Sayyah, A.; Aflaki, M. & Rezazadeh, A. R. (2006). GA-based optimization of total harmonic current distortion and suppression of chosen harmonics in induction motors, *Proceedings of international symposium on power electronics, electrical drives, automation and motion*, pp. 1361-1366, Italy, May 2006, Taormina (Sicily)

Sayyah, A.; Aflaki, M. & Rezazadeh, A. R. (2006). Optimal PWM for minimization of total harmonic current distortion in high-power induction motors using genetic algorithms, *Proceedings of SICE-ICASE international joint conference*, Korea, pp. 5494-5499, October 2006, Busan.

Sayyah, A.; Aflaki, M. & Rezazadeh, A. R. (2006). Optimization of THD and suppressing certain order harmonics in PWM inverters using genetic algorithms, *Proceedings of IEEE international symposium on intelligent control*, pp. 874-879, Germany, October 2006, Munich.

Sun, J. (1995). *Optimal Pulsewidth Modulation Techniques for High Power Voltage-source Inverters*, Thesis, University of Paderborn, Germany.

Sun, J.; Beineke, S. & Grotstollen, H.: (1996). Optimal PWM based on real-time solution of harmonic elimination equations. it IEEE Transactions on Power Electronics, Vol. 11, No. 4, July 1996, 612-621.

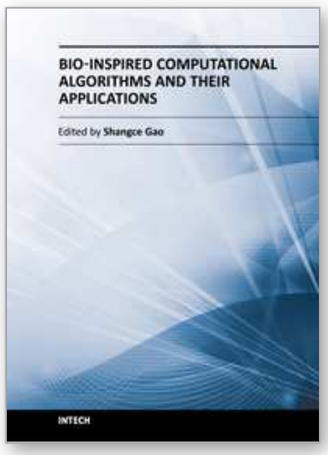

Bio-Inspired Computational Algorithms and Their Applications
Edited by Dr. Shangce Gao

ISBN 978-953-51-0214-4
Hard cover, 420 pages
Publisher InTech
Published online 07, March, 2012
Published in print edition March, 2012

Bio-inspired computational algorithms are always hot research topics in artificial intelligence communities. Biology is a bewildering source of inspiration for the design of intelligent artifacts that are capable of efficient and autonomous operation in unknown and changing environments. It is difficult to resist the fascination of creating artifacts that display elements of lifelike intelligence, thus needing techniques for control, optimization, prediction, security, design, and so on. Bio-Inspired Computational Algorithms and Their Applications is a compendium that addresses this need. It integrates contrasting techniques of genetic algorithms, artificial immune systems, particle swarm optimization, and hybrid models to solve many real-world problems. The works presented in this book give insights into the creation of innovative improvements over algorithm performance, potential applications on various practical tasks, and combination of different techniques. The book provides a reference to researchers, practitioners, and students in both artificial intelligence and engineering communities, forming a foundation for the development of the field.

INTECH
open science | open minds

InTech Europe
University Campus STeP Ri
Slavka Krautzeka 83/A
51000 Rijeka, Croatia
Phone: +385 (51) 770 447
Fax: +385 (51) 686 166
www.intechopen.com

InTech China
Unit 405, Office Block, Hotel Equatorial Shanghai
No.65, Yan An Road (West), Shanghai, 200040, China
中国上海市延安西路65号上海国际贵都大饭店办公楼405单元
Phone: +86-21-62489820
Fax: +86-21-62489821

IntechOpen